

THE PLANE $W(\text{Na I}) \times W(\text{Mg I})$: EFFECTS OF INTERSTELLAR Na I IN A SAMPLE OF SOUTHERN GALAXIES

E. BICA AND M. G. PASTORIZA

Departamento de Astronomia, Instituto de Física, UFRGS, Caixa Postal 15051, Porto Alegre 91500, RS, Brazil

M. MAIA

Observatório Nacional/CNPq, Rua Gal. José Cristino 77, Rio de Janeiro, 20921, RJ, Brazil

L. A. L. DA SILVA AND H. DOTTORI

Departamento de Astronomia, Instituto de Física, UFRGS, Caixa Postal 15051, Porto Alegre 91500, RS, Brazil

Received 5 February 1991; revised 17 July 1991

ABSTRACT

Galaxy spectra from a subsample of the Southern Sky Redshift Survey data bank were used to study the equivalent width plane for the lines Na I λ 5893 Å vs Mg I λ 5175 Å. We try to estimate how important the contribution of the interstellar gas for the sodium line is compared to that of the stellar population. The sample is made up of galaxies with morphological types from E to Sc and are distributed up to radial velocities of 25 000 km s⁻¹, most of them smaller than 15 000 km s⁻¹. Most early type galaxies with dust lanes, particularly nearly edge-on SO's, present an enhancement of the Na I line. Inclined spiral galaxies tend to present enhanced Na I with respect to face-on spirals. This tendency, previously found in a smaller sample of galaxies limited to $V < 6000$ km s⁻¹, is now confirmed for more distant ones. In the large velocity sample we are observing the global bulge rather than the very nucleus; the persistence of the effect suggests that the scale height of the gas layer in the central disk can reach a considerable fraction of the bulge radius.

1. INTRODUCTION

In the interstellar medium (ISM), gas and dust grains are generally associated, as inferred from the correlations between the intensity of the interstellar Na I doublet (5893 Å) and the reddening of starlight (Spitzer 1948; Hobbs 1974). This property has been extensively used to probe the Galactic ISM (e.g., Cohen 1973).

The behavior of the Na I line in a sample of globular and open Galactic and Magellanic Cloud clusters as well as nearby galaxies, as a function of reddening, was investigated by Bica & Alloin (1986). In particular, they have studied the age and metallicity effects which affect the position of a galaxy in the $W(\text{Na I}) \times W(\text{Mg I})$ plane, as a function of factors such as the inclination and morphological type. They have found that the Na I (λ 5893 Å) is enhanced with inclination in spirals. Also the very metallic early type galaxies seem to deviate from a linear relationship in the $W(\text{Na I}) \times W(\text{Mg I})$ plane. The main conclusion was that the Na I D lines show a strong contamination by the interstellar gas contribution.

In this paper we investigate the effects of the interstellar Na I in a larger sample of southern galaxies, on average more distant, in order to disentangle in different types of galaxies the interstellar gas contribution from that of the stellar population. In Sec. 2 we discuss the data sources and their processing. The analysis is presented in Sec. 3 and the conclusions in Sec. 4.

2. THE DATA

The data basis for this work is the Southern Sky Redshift Survey (SSRS) data bank (see da Costa *et al.* 1989, and references therein). It contains not only spectra of galaxies which belong to the SSRS survey, but also for some galaxies in the Hydra-Centaurus region, and in the remaining of the

southern polar cap not covered by the SSRS survey. The galaxy distribution in the sky is not homogeneous or complete to any criteria, but this is not supposed to affect the results of this study. The SSRS survey used a photon-counting Reticon detector mounted on the 1.5 m telescope of the Laboratório Nacional de Astrofísica, Brasópolis, Brazil and on the CASLEO 2.14 m telescope in San Juan, Argentina. The spectra have a typical resolution of 6 Å, and cover the spectral region of λ 4700– λ 7100 Å.

The software used for data reduction (da Costa *et al.* 1984) provides the radial velocities and also the equivalent widths (W) of the more prominent emission and absorption lines. At the employed resolution the Na I doublet lines D_1 (λ 5896 Å) and D_2 (λ 5890 Å), as well as the Mg I triplet ones b_4 (λ 5167 Å), b_2 (λ 5173 Å), and b_1 (λ 5184 Å), are still blended (see Fig. 1 for examples). The equivalent widths $W(\text{Na I})$ and $W(\text{Mg I})$ for the present sample measure the global absorption in each case.

We have examined almost 2000 spectra, looking for those with a good signal-to-noise ratio for a stellar population analysis. The final sample, for which the basic galaxy parameters could be found in the literature, contains 736 galaxies. The sample contains galaxies with morphological types from E to Sc with velocities smaller than 25 000 km s⁻¹ (most of them smaller than 15 000 km s⁻¹).

The dataset is presented in Tables 1–3 for galaxies having IC, NGC, and ESO numbers, respectively. For each galaxy in these tables, we give the following information: in column 1 the galaxy's catalog (IC, NGC, or ESO) number, in column 2 its morphological type, in columns 3 and 4 the measured equivalent width of Mg I (λ 5175 Å) and the error associated to it, respectively, in columns 5 and 6 the same parameters for Na I (λ 5890 Å) absorption line, and the last column (7) contains the galaxy axial ratio b/a .

The morphological type and the b/a ratios for the galaxies

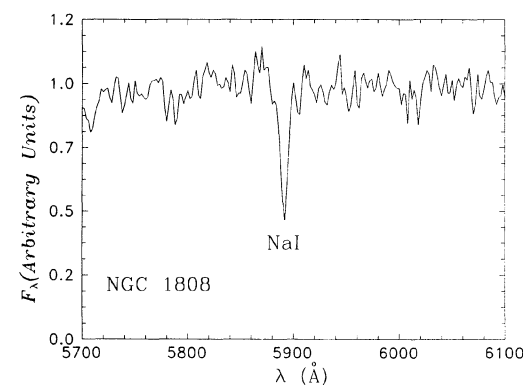
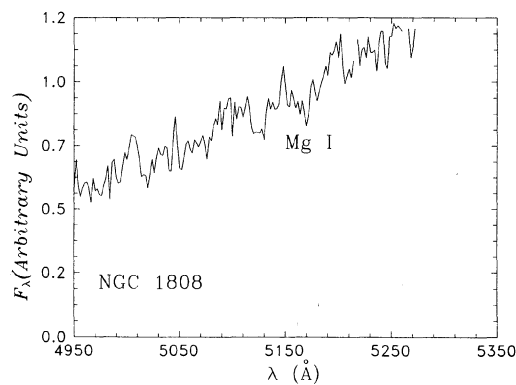
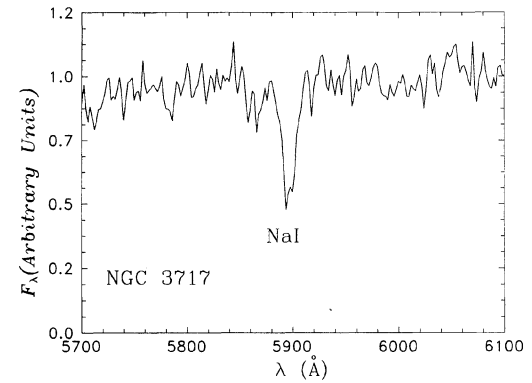
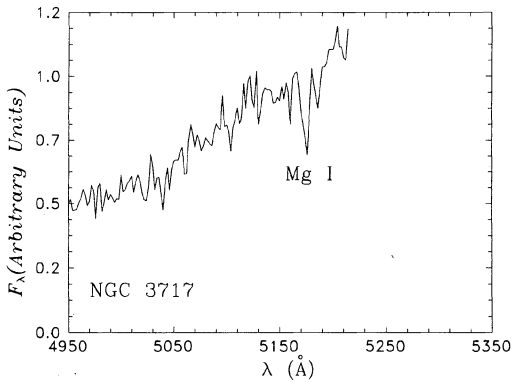
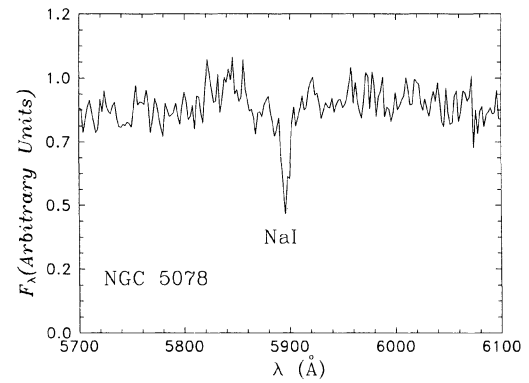
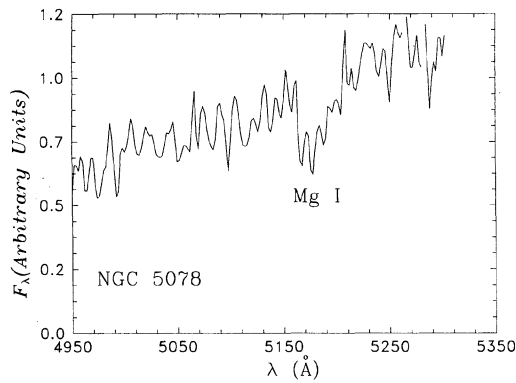
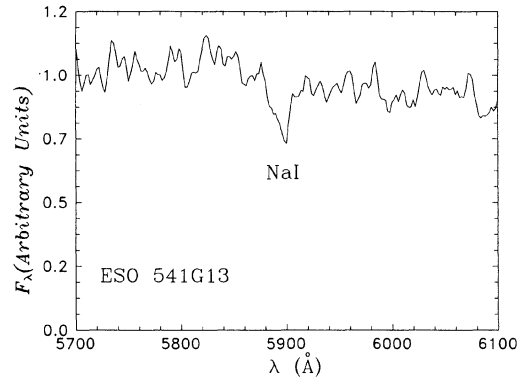
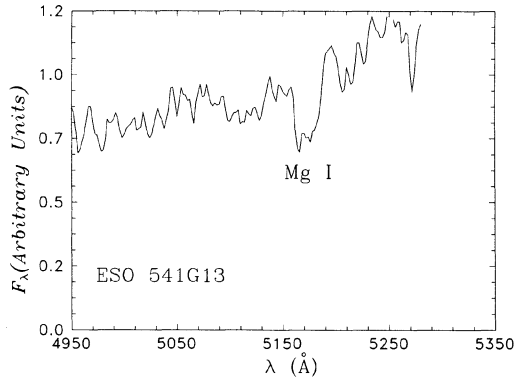


FIG. 1. Enlargements of the Mg I and Na I spectral regions for the galaxies ESO 541 G13, NGC 5078, NGC 3717, and NGC 1808 (see Secs. 2 and 3 for details).

TABLE 1. Data for IC galaxies.

GALAXY IC	TYPE	W(Mg I) $\pm \sigma$ (5175Å)	W(Na I) $\pm \sigma$ (5890Å)	b/a	GALAXY IC	TYPE	W(Mg I) $\pm \sigma$ (5175Å)	W(Na I) $\pm \sigma$ (5890Å)	b/a
844	-2	2.0 0.9	2.7 0.5	0.25	4323	3	4.9 0.8	3.4 0.6	0.08
874	-2	2.6 1.2	3.8 0.7	0.86	4329	-3	3.0 0.6	5.6 0.1	0.45
1386	-5	3.3 0.9	4.6 0.6	0.76	4350	-2	4.6 1.0	5.4 0.6	0.53
1439	1	3.3 1.1	3.5 0.6	0.71	4352	0	2.3 1.3	4.9 0.7	0.40
1443	-2	3.3 1.1	4.3 0.7	0.82	4367	5	5.9 1.1	3.5 0.8	1.00
1445	-3	5.4 1.0	2.9 0.6	0.88	4374	-2	4.3 1.0	5.9 0.7	0.93
1531	-2	5.1 1.2	3.9 0.8	0.81	4937	-2	2.6 1.7	2.6 1.1	0.19
1587	-2	3.2 2.0	4.1 0.9	0.29	4944	-2	3.2 1.0	2.8 0.8	0.35
1608	1	4.0 1.0	5.0 0.6	0.43	4975	-2	3.0 1.2	4.0 0.0	0.92
1615	3	5.7 1.6	2.3 0.9	0.43	4991	-2	5.3 0.6	4.2 0.7	0.64
1625	-3	6.4 1.1	5.1 0.7	0.89	4994	0	3.9 1.6	5.3 0.8	0.92
1633	-2	4.4 0.8	5.1 0.6	0.96	4995	-2	2.7 1.4	3.2 0.8	0.67
1657	3	2.3 0.3	3.4 0.5	0.25	4998	5	3.5 1.6	4.3 1.0	0.85
1719	-2	4.4 1.3	4.9 1.0	0.71	5011	-2	2.1 0.6	4.0 0.5	0.53
1729	-3	5.0 1.0	2.3 0.8	0.48	5019	3	3.6 1.6	4.6 1.1	0.20
1759	1	2.3 1.5	2.5 0.9	1.00	5020	5	2.6 1.4	3.0 0.9	0.71
1783	3	2.2 1.5	3.4 0.8	0.43	5064	1	3.9 1.8	2.8 1.0	0.57
1812	-2	6.9 1.1	4.8 0.7	0.91	5065	-2	1.8 0.2	3.3 0.5	0.88
1858	-2	2.9 1.2	3.0 0.8	0.28	5071	3	4.9 1.1	4.0 0.9	0.28
1860	-5	4.8 2.6	3.5 1.3	0.74	5084	1	2.6 1.1	3.9 0.4	0.67
1864	-5	3.8 0.8	4.5 0.6	0.57	5088	1	5.7 1.2	3.9 0.8	1.00
1875	-5	5.3 1.1	2.8 0.8	1.00	5094	1	2.5 1.6	3.9 1.1	0.67
1909	2	4.4 1.0	4.0 0.7	0.54	5096	3	3.4 1.2	3.3 0.6	0.15
1928	1	2.5 1.1	4.7 0.7	0.25	5105	-3	2.9 1.3	5.9 0.7	0.67
2006	-3	4.2 0.9	4.0 0.7	0.84	5105A	5	1.9 1.5	3.6 1.1	0.75
2035	-5	2.3 0.6	2.7 0.4	0.73	5128	0	3.0 1.0	1.6 0.7	0.58
2051	5	4.6 1.2	3.2 0.9	0.63	5131	-2	4.8 0.9	3.3 0.6	1.00
2082	9	5.2 1.2	3.7 0.8	0.67	5139	-2	4.9 0.8	3.9 0.6	0.46
2122	-2	4.6 0.3	4.2 0.4	0.92	5141	3	3.0 1.0	1.9 0.8	0.78
2627	5	2.5 1.0	1.4 0.9	0.85	5156	3	3.1 1.5	3.2 0.8	0.33
2764	-2	3.1 1.2	2.9 0.8	0.92	5157	-3	3.4 0.9	4.6 0.6	1.00
4180	-2	3.1 1.1	2.4 0.6	0.88	5170	3	1.5 0.9	3.3 0.8	0.45
4197	-5	5.9 1.2	3.4 0.7	0.60	5181	-2	3.9 1.7	5.2 0.4	0.36
4214	-2	3.8 0.5	3.2 0.4	0.63	5186	1	3.4 0.8	4.2 0.6	0.69
4252	-2	5.5 1.1	5.0 0.8	0.63	5210	-2	4.0 1.3	3.9 0.7	0.90
4253	3	3.7 1.1	4.1 0.8	0.39	5211	1	5.8 1.1	4.4 0.7	0.73
4255	-3	5.1 1.0	5.4 1.1	0.62	5244	10	3.9 1.0	5.1 0.4	0.17
4262	2	2.2 1.7	4.4 1.0	0.27	5262N	9	3.9 1.2	4.3 0.7	0.67
4281	3	5.4 2.0	7.1 1.1	0.87	5269	-2	4.0 0.2	2.0 0.2	0.41
4288	11	2.9 1.4	4.9 0.8	0.44	5290	3	2.5 1.1	2.6 0.7	0.62
4290	1	3.9 4.5	2.7 1.1	0.81	5321	3	3.8 1.6	1.6 1.2	0.63
4293	-3	5.2 1.2	4.0 0.8	0.76	5323	0	3.0 1.0	4.8 0.7	0.68
4298	4	5.2 1.4	3.1 0.9	0.53	5353	-3	5.7 1.0	4.0 0.8	0.86
4310	-2	6.4 1.2	4.4 0.7	0.40	5362	-3	3.3 1.4	5.7 0.9	1.00
4320	-12	2.2 1.5	4.2 0.9	1.00					

TABLE 2. Data for NGC galaxies.

GALAXY NGC	TYPE (5175Å)	W(Mg I) ± σ (5890Å)	W(Na I) ± σ	b/a	GALAXY NGC	TYPE (5175Å)	W(Mg I) ± σ (5890Å)	W(Na I) ± σ	b/a
10	5	6.0 1.3	4.3 1.0	0.56	1291	0	4.2 0.5	5.2 0.3	1.00
98	1	4.9 1.0	3.7 0.8	0.78	1315	-2	4.1 0.9	2.9 0.6	0.94
177	1	2.7 1.1	4.9 0.6	0.23	1316	-12	4.1 0.5	4.9 0.3	0.74
179	-5	1.4 0.8	4.2 0.5	0.71	1317	0	4.6 0.8	3.9 0.6	0.89
209	-2	4.9 1.0	3.6 0.7	0.93	1319	1	4.3 1.1	2.6 0.6	0.44
215	-3	3.7 1.4	4.5 0.8	0.73	1326	0	2.3 0.7	3.5 0.5	0.72
254	-2	3.5 0.7	2.1 0.5	0.48	1329	1	3.4 1.4	6.0 0.8	0.93
312	-5	4.0 0.9	3.3 0.6	0.87	1336	-2	2.8 1.1	3.4 0.6	0.78
322	1	1.8 1.5	5.3 0.8	0.50	1339	-5	4.4 0.9	5.4 0.6	0.87
324	-2	2.9 1.2	3.6 0.7	0.29	1340	-5	4.4 0.6	4.5 0.5	0.70
360	5	5.4 1.4	4.2 1.4	0.15	1351	-2	4.5 0.9	2.7 0.6	0.63
415	3	3.6 1.6	3.3 1.0	0.59	1352	0	3.7 0.9	2.3 0.5	0.64
439	-3	4.6 1.1	4.4 0.7	0.62	1362	-2	4.6 1.0	3.2 0.6	0.93
441	0	5.4 1.7	3.6 1.1	0.75	1365	5	0.3 0.9	4.4 0.6	0.55
491	3	4.2 1.0	2.0 0.7	0.91	1370	-2	0.2 1.1	1.9 0.7	0.65
527	1	3.9 0.9	4.5 0.6	0.24	1374	-2	5.6 0.9	5.4 0.6	0.98
534	-2	4.0 1.0	4.0 0.7	0.82	1377	-2	1.3 1.3	3.3 0.7	0.43
545	-2	5.0 1.5	4.6 0.9	0.68	1379	-5	3.6 0.7	3.1 0.6	0.95
547	-5	3.5 1.5	5.0 1.0	0.93	1381	-2	4.3 0.7	3.4 0.4	0.23
568	-2	5.3 1.2	4.7 0.7	0.59	1389	-2	3.9 0.6	3.6 0.4	0.65
597	5	2.5 1.3	2.4 1.1	1.00	1393	-2	2.5 1.2	3.3 0.6	0.85
641	-5	2.7 1.6	4.8 0.8	1.00	1399	-5	6.2 0.7	6.6 0.5	0.95
686	-2	4.8 1.1	4.7 0.7	0.87	1400	-3	3.0 1.0	4.6 0.6	0.87
692	5	4.9 1.0	2.8 0.6	1.00	1401	-2	3.9 0.9	3.1 0.5	0.29
696	0	4.8 1.3	5.2 0.8	0.40	1403	-5	4.4 1.0	4.4 0.6	0.67
723	1	1.4 1.0	1.6 0.6	0.88	1404	-5	4.6 1.1	4.8 0.1	0.93
727	-2	5.5 1.2	3.6 0.8	0.69	1407	-3	3.4 1.0	4.2 0.6	1.00
731	-5	4.4 0.7	4.6 0.6	1.00	1416	-2	4.7 1.8	3.4 0.8	1.00
749	1	2.3 0.9	3.5 0.5	0.80	1419	-5	4.1 0.9	2.7 0.7	1.00
822	-5	5.2 1.0	3.6 0.7	0.54	1426	-5	4.6 1.1	4.4 0.6	0.68
824	3	4.1 0.9	2.3 0.8	0.95	1427	-2	3.6 0.8	2.8 0.5	0.69
854	3	2.6 1.0	2.1 0.8	0.36	1439	-5	4.4 0.8	5.3 0.6	0.93
857	10	2.8 1.3	4.3 0.8	0.88	1482	11	4.0 1.6	5.2 0.9	0.60
862	-3	5.1 1.0	3.0 1.0	1.00	1489	3	3.2 1.2	2.2 1.0	0.44
872	5	3.7 2.3	2.8 1.3	0.77	1537	-5	4.3 0.8	4.6 0.7	0.67
889	-2	4.7 1.0	4.2 0.6	0.85	1543	-2	4.7 0.9	5.4 0.7	0.52
893	4	5.0 1.5	2.8 1.0	0.75	1547	3	2.6 1.7	3.5 0.9	0.50
897	1	4.1 1.1	4.3 0.7	0.68	1558	3	3.3 1.2	2.5 0.7	0.37
936	-2	5.1 0.8	4.4 0.6	0.79	1559	5	1.5 1.6	1.8 1.0	0.59
939	0	5.8 1.1	3.5 0.8	0.85	1566	5	3.7 0.7	1.7 0.5	0.79
964	2	4.2 0.9	5.4 0.7	0.24	1567	-2	2.9 0.7	4.4 0.5	1.00
967	-2	6.5 1.0	3.9 0.8	0.62	1571	-2	2.1 1.4	4.4 0.4	0.83
1091	1	2.9 0.9	4.0 0.7	0.80	1572	3	2.9 1.0	3.7 0.8	0.50
1092	-2	3.5 0.9	4.4 0.7	0.78	1631	0	3.8 1.4	3.6 0.8	0.70
1097	3	2.3 0.7	4.9 0.5	0.68	1672	5	2.4 0.3	3.3 0.2	0.78
1098	-2	2.7 1.3	5.0 0.7	0.93	1668	-2	3.6 0.9	4.4 0.6	0.50
1099	3	4.3 1.2	5.1 0.7	0.35	1700	-5	3.4 0.6	4.4 0.4	0.68
1100	1	3.5 1.7	2.9 0.9	0.45	1784	4	3.4 1.2	2.3 0.7	0.65
1165	1	2.9 1.1	4.3 0.9	0.34	1808	11	2.2 0.8	7.2 0.5	0.52
1201	-5	4.1 0.6	5.0 0.4	0.59	1947	-12	1.1 1.2	6.6 0.9	0.85
1209	-5	3.5 0.9	4.8 0.6	0.52	2207	9	3.7 0.6	3.6 0.4	0.66
1217	2	5.1 0.7	4.1 0.8	0.75	2223	5	3.6 0.8	3.2 0.7	0.85
1228	-2	2.9 2.3	4.0 1.1	0.59	3115	-3	4.6 0.6	5.3 0.4	0.33
1256	-2	2.4 1.3	4.8 0.7	0.38	3145	4	3.8 0.5	4.3 0.4	0.51

TABLE 2. (continued)

GALAXY NGC	TYPE (5175Å)	W(Mg I) ± σ (5890Å)	W(Na I) ± σ	b/a	GALAXY NGC	TYPE (5175Å)	W(Mg I) ± σ (5890Å)	W(Na I) ± σ	b/a
3166	0	4.8 0.8	5.3 0.5	0.55	6070	5	2.3 1.4	3.7 0.5	0.55
3379	-5	5.4 0.7	5.2 0.5	0.85	6814	4	5.8 1.7	1.6 1.1	0.91
3557	-5	4.5 1.0	5.0 0.1	0.65	6835	1	1.1 0.9	1.7 0.8	0.18
3717	13	3.6 0.9	5.9 0.6	0.26	6848	-2	3.3 0.7	5.1 0.5	0.35
4030	4	3.0 0.6	3.7 0.6	0.72	6851	-2	3.9 0.4	4.1 0.1	0.71
4304	5	1.5 0.9	4.5 0.8	0.98	6855	-2	5.7 0.6	4.4 0.5	1.00
4374	-5	6.5 0.8	4.8 0.5	0.83	6860	1	2.8 1.2	2.7 0.7	0.54
4406	-5	5.9 0.7	4.5 0.4	0.69	6861	-2	4.9 0.7	4.0 0.5	0.27
4472	-5	4.2 0.7	5.4 0.5	0.81	6868	-5	4.8 0.4	5.5 0.9	0.81
4486	-5	3.6 1.4	6.6 0.8	0.93	6875	-2	4.6 0.9	3.6 0.6	0.47
4553	-2	4.4 1.1	3.3 0.7	0.46	6893	-2	5.9 0.7	4.6 0.5	0.63
4696	-2	4.6 1.1	4.3 0.9	0.91	6899	5	3.0 1.0	2.7 0.8	0.61
4831	-2	2.5 1.0	3.5 0.7	0.50	6909	-5	3.6 0.6	2.2 0.4	0.49
4905	1	4.4 1.1	4.7 0.7	0.93	6935	1	3.9 1.4	2.8 0.9	0.85
4939	4	5.9 0.9	3.7 0.5	0.54	6948	3	1.8 1.0	2.9 0.7	0.48
4955	-3	4.6 1.3	4.8 0.7	0.78	6958	-5	3.7 0.5	3.4 0.4	0.91
4968	-2	4.8 1.6	3.5 0.8	0.56	7002	-5	4.8 0.9	5.1 0.7	0.86
4970	-2	4.6 0.9	3.4 0.6	0.54	7007	-2	4.4 0.6	3.6 0.4	0.60
4993	-3	4.3 1.2	2.8 0.7	0.83	7014	-3	3.2 1.3	5.6 0.7	1.00
5048	-3	4.1 1.0	2.6 0.6	0.39	7035	-2	4.1 1.7	4.0 0.9	0.50
5062	-2	4.6 0.9	5.4 0.6	0.32	7035	-2	5.2 1.5	4.1 0.9	0.50
5078	-12	4.4 1.1	7.2 0.6	0.42	7041	-2	3.5 0.8	2.7 0.0	0.35
5101	0	5.0 0.1	4.5 0.8	0.83	7049	-2	3.9 0.6	5.6 0.4	0.76
5108	1	5.4 1.4	3.7 0.9	0.27	7057	-2	5.7 1.5	4.2 0.8	0.59
5126	-12	1.8 1.4	3.8 0.7	0.33	7060	1	3.7 0.9	4.7 0.8	0.57
5134	3	2.3 0.5	2.6 0.4	0.54	7075	-3	5.7 1.3	4.8 0.7	0.71
5135	1	3.3 0.5	2.3 0.5	0.43	7097	-5	3.5 1.0	4.3 0.8	0.56
5153	-5	3.5 1.3	4.7 0.7	0.71	7103	0	4.7 1.0	3.6 0.6	1.00
5161	5	5.5 1.6	2.3 1.3	0.36	7109	-2	2.7 0.8	2.4 0.7	1.00
5215A	9	3.9 1.1	2.8 0.6	0.50	7110	3	3.7 1.2	1.7 0.7	0.60
5215B	9	2.4 1.0	3.3 0.7	0.33	7123	-12	4.9 1.3	6.5 0.7	0.40
5298	3	6.4 1.8	3.8 1.0	0.68	7145	-2	4.2 1.3	4.1 1.8	1.00
5393	1	4.5 1.1	2.6 0.7	0.83	7155	0	3.3 1.2	3.8 0.8	0.59
5397	-2	4.5 1.4	3.4 0.8	0.56	7166	-2	3.6 0.7	4.4 0.5	0.39
5419	-2	4.1 1.9	5.2 0.6	0.86	7168	-3	4.3 0.7	4.0 0.6	0.79
5495	5	3.0 1.2	3.3 0.8	0.90	7172	-12	3.7 1.4	4.7 0.9	0.56
5576	-5	4.3 0.4	3.5 0.3	0.65	7173	3	5.3 0.7	3.6 0.5	0.66
5643	5	3.3 0.5	2.4 0.6	0.89	7176	3	5.2 0.8	4.5 0.5	0.85
5734	10	1.2 1.2	6.6 0.8	0.67	7180	-5	3.7 0.8	2.9 0.7	0.50
5740	3	4.0 1.2	2.7 0.9	0.50	7185	-2	4.6 0.6	2.1 0.4	0.69
5746	3	3.8 1.6	6.8 0.1	0.19	7187	-2	4.1 0.8	2.7 0.6	0.89
5761	-2	1.5 1.2	3.8 0.7	0.94	7201	1	2.7 1.1	3.3 0.6	0.33
5770	-2	2.7 0.7	2.3 0.5	0.81	7203	1	4.3 1.1	3.9 0.8	0.52
5791	-2	4.1 1.0	4.2 0.6	0.56	7213	-2	4.5 0.5	3.7 0.3	0.95
5792	3	2.6 1.2	6.2 0.9	0.27	7220	-2	2.0 0.9	2.6 0.6	0.73
5796	-5	4.7 0.5	6.1 0.5	0.83	7221	3	2.4 1.7	2.8 0.9	0.78
5806	3	3.9 0.7	3.7 0.5	0.57	7225	-12	3.7 1.2	6.0 0.8	0.52
5813	-5	4.3 0.8	5.0 0.5	0.76	7232	0	5.3 1.0	5.2 0.6	0.25
5831	-5	4.5 1.2	4.6 0.8	0.89	7236	9	3.3 1.2	3.8 0.8	0.57
5839	-2	3.8 0.9	5.9 0.6	1.00	7237	-2	4.4 1.0	4.1 0.7	0.57
5845	-5	3.5 0.6	4.0 0.4	1.00	7262	1	3.4 1.1	3.4 0.9	1.00
5846	-5	5.8 1.0	5.7 0.4	0.91	7289	-2	6.4 0.9	3.8 0.7	0.78
5915	2	0.9 0.4	1.3 0.4	0.12	7358	-2	4.5 0.7	3.3 0.1	0.30
5921	3	1.9 0.6	3.3 0.4	0.83	7359	-2	5.1 1.2	2.8 0.8	0.24

TABLE 2. (continued)

GALAXY NGC	TYPE (5175Å)	W(Mg I) ± σ (5890Å)	W(Na I) ± σ	b/a	GALAXY NGC	TYPE (5175Å)	W(Mg I) ± σ (5890Å)	W(Na I) ± σ	b/a
7365	-5	1.0 1.2	2.7 0.8	0.77	7626	-5	4.2 1.1	5.7 0.7	0.89
7377	1	2.7 1.1	4.0 0.5	0.79	7632	-2	3.5 1.3	5.0 0.9	0.50
7382	1	3.7 1.5	4.4 0.8	0.29	7633	-2	4.8 0.7	4.8 0.6	0.80
7404	-3	2.8 0.7	2.4 0.6	0.55	7676	-5	4.3 1.5	3.9 0.8	0.43
7417	0	3.8 0.9	2.8 0.6	0.69	7702	-2	5.7 0.9	3.7 0.6	0.58
7421	4	3.0 1.5	1.8 0.9	0.89	7733	9	3.8 1.2	3.7 0.3	0.58
7484	-2	4.5 0.6	5.1 0.5	1.00	7736	-2	4.9 1.5	3.7 0.2	1.00
7507	-3	4.9 0.7	5.7 0.6	1.00	7742	3	3.2 1.1	2.5 0.7	1.00
7552	3	2.2 0.3	4.4 0.2	0.67	7744	-2	5.3 0.6	5.5 0.4	0.76
7562	-5	5.1 1.2	5.1 0.7	0.65	7758	-2	7.2 1.2	5.1 0.9	0.64
7582	4	2.1 1.1	5.3 0.6	0.32	7785	-5	5.5 1.1	4.7 0.6	0.54
7619	-5	4.7 2.4	5.1 0.0	0.91	7796	-5	4.8 0.8	5.5 0.5	0.85

TABLE 3. Data for ESO galaxies.

GALAXY ESO	TYPE	W(Mg I) ± σ (5175Å)	W(Na I) ± σ (5890Å)	b/a	GALAXY ESO	TYPE	W(Mg I) ± σ (5175Å)	W(Na I) ± σ (5890Å)	b/a
003-01	-2	2.5 0.9	3.1 0.8	1.00	202-01	-2	4.0 0.8	3.2 0.6	0.71
015-05	2	3.2 1.1	2.2 0.8	0.83	202-15	0	4.4 0.7	4.6 0.6	1.00
030-11	-2	4.6 1.1	4.0 0.8	0.68	203-15	4	3.2 2.3	3.8 1.2	0.46
031-05	3	1.7 1.6	3.4 1.4	0.43	204-06	1	7.8 2.1	4.1 1.2	0.46
033-04	2	4.4 1.1	2.1 0.9	0.72	204-13	10	3.1 2.6	3.7 1.1	0.36
075-28	-2	5.1 0.7	4.6 0.5	0.74	234-11	1	4.7 2.0	3.9 0.9	0.44
107-04	-5	3.8 0.7	4.3 0.5	0.73	234-51	-2	4.5 1.2	5.2 0.7	0.71
107-44	-2	5.2 1.1	2.8 0.7	0.67	235-33	3	3.1 1.2	1.7 0.9	0.82
110-27	-2	5.2 1.4	3.8 0.7	0.43	235-49	-5	2.9 0.7	4.2 0.6	0.63
114-14	1	3.4 1.7	2.7 1.2	0.90	235-50	-2	5.5 1.1	5.3 0.9	0.70
114-16	1	4.0 1.1	4.6 0.8	0.70	235-55	1	2.9 1.2	4.7 0.7	1.00
119-25	1	4.8 1.1	4.7 0.7	0.47	235-58	1	3.4 2.3	6.2 1.4	0.76
142-49	-2	4.4 1.1	4.2 0.6	0.62	235-84	0	3.1 1.9	3.6 1.3	0.88
146-28	-2	3.4 1.5	4.6 0.8	0.80	237-28	-2	4.0 1.0	3.8 0.7	0.40
148-17	-2	2.0 0.5	2.6 0.6	0.32	240-11	5	5.9 1.0	5.1 1.3	0.10
149-12	-3	4.6 1.8	5.3 1.0	0.42	241-23	3	2.8 1.3	3.8 0.8	0.48
152-26	1	5.4 1.5	2.8 0.8	0.70	243-35	-2	4.7 1.2	4.4 0.8	0.91
153-27	-2	3.7 1.0	3.6 0.8	0.35	243-37	-2	4.8 1.0	3.3 0.7	0.67
154-10	1	3.7 1.2	7.6 1.0	0.40	243-51	1	5.3 1.2	3.2 0.8	0.60
156-18	-2	4.0 0.9	2.8 0.8	0.41	244-23	11	3.1 1.5	5.0 0.8	0.15
159-03	-2	4.6 0.8	3.1 0.6	0.54	244-39	1	3.3 1.4	4.4 0.9	0.33
185-25	-2	4.4 1.4	3.7 0.9	0.67	246-15	1	3.3 1.0	2.4 0.7	0.40
185-27	-3	2.0 1.2	4.0 0.6	0.70	246-16	0	2.9 1.4	3.9 0.9	0.40
185-54	-2	5.2 1.5	3.4 1.3	0.69	246-21	2	5.2 1.0	4.6 0.8	0.62
185-64	0	5.8 2.2	3.2 1.1	0.43	251-01	9	1.7 1.1	2.5 0.8	0.58
187-20	8	4.9 0.4	6.7 1.5	0.92	252-10	2	3.4 1.2	3.1 0.9	0.80
187-59	-2	4.4 2.0	2.8 0.8	0.57	284-07	1	2.6 1.8	3.7 0.9	0.18
188-19	9	4.9 1.3	5.2 1.0	0.30	284-09	-2	2.5 1.2	3.3 0.7	0.46
189-12	5	5.6 1.4	5.2 1.0	0.11	284-17	-2	7.6 2.7	4.6 1.1	0.50
193-09	1	3.7 1.1	2.5 0.8	0.29	284-23	-2	4.0 0.5	3.4 0.4	1.00
193-26	-2	3.5 1.3	5.4 0.7	0.58	284-32	1	4.2 1.4	2.9 0.9	1.00
194-04	0	2.1 1.4	2.4 0.8	0.33	284-38	-2	2.0 1.8	4.6 0.8	0.47
196-03	0	3.3 1.7	4.1 1.8	0.82	284-41	9	4.0 0.3	2.6 1.8	0.80
197-18	-2	4.4 0.7	3.8 0.5	0.53	284-44	-2	4.1 1.4	3.3 0.7	0.52
198-02	0	3.9 1.5	3.2 0.7	0.55	285-20	3	3.8 1.2	2.9 1.0	0.59
198-19	-2	5.2 2.0	3.9 1.1	0.67	285-49	1	6.1 1.5	4.3 1.8	0.43
199-01	1	3.4 1.3	2.2 0.7	0.92	286-10	0	4.0 1.1	3.9 0.8	0.83
199-21	8	3.2 1.7	4.0 0.9	0.78	286-37	-2	3.2 1.7	4.5 0.9	0.31
201-21	0	4.4 1.6	3.8 0.9	0.40	286-41	-2	3.3 1.2	4.4 0.9	0.58

TABLE 3. (continued)

GALAXY	TYPE	W(Mg I) \pm σ	W(Na I) \pm σ	b/a	GALAXY	TYPE	W(Mg I) \pm σ	W(Na I) \pm σ	b/a
ESO		(5175Å)	(5890Å)		ESO		(5175Å)	(5890Å)	
286-49	-5	5.6 0.8	5.1 0.6	0.63	346-32	-2	4.7 1.0	4.3 0.8	1.00
286-50	-5	2.8 0.8	1.9 0.5	0.50	347-13	11	4.6 1.4	2.7 1.1	0.17
286-59	-5	4.0 2.4	4.7 1.1	0.58	347-29	6	2.0 1.3	2.7 2.0	0.50
287-07	-2	4.7 1.4	4.7 0.9	0.75	348-06	-2	4.1 0.9	3.6 0.7	0.70
287-16	3	3.9 0.9	4.2 0.6	1.00	348-10	-2	4.0 1.5	2.0 1.0	0.71
287-35	1	4.7 2.3	3.1 1.0	0.50	349-01	-2	5.8 1.5	5.7 1.0	0.90
290-10	9	6.7 1.6	4.1 0.9	0.38	349-06	3	3.8 1.2	2.4 1.3	0.70
290-51	9	2.3 1.2	3.8 1.1	0.60	349-09	3	4.4 1.7	4.0 1.1	0.77
291-04	1	4.4 1.5	3.2 0.9	0.35	349-13	-2	6.6 1.0	4.1 1.0	0.60
292-07	-2	4.5 2.0	6.0 2.0	0.69	349-18	0	2.8 1.1	2.9 0.8	0.67
292-09	3	6.2 1.8	4.2 1.3	0.28	349-19	1	5.2 2.8	2.7 1.7	0.92
292-22	-2	3.1 2.4	3.8 1.0	0.59	349-22	-2	6.0 1.4	5.8 1.1	1.00
293-13	1	3.2 2.2	2.5 1.0	1.00	349-30	3	5.3 1.4	3.0 1.3	0.50
295-22	9	6.1 2.1	6.7 1.7	0.50	349-38	3	3.8 1.1	4.8 0.8	0.50
296-28	1	2.1 1.0	3.9 0.9	0.58	350-01	3	5.5 1.5	2.7 1.6	0.80
297-06	1	5.0 1.3	3.6 0.8	0.92	350-04	1	2.7 1.0	2.7 0.8	0.70
297-09	-2	3.8 1.0	2.9 0.9	1.00	350-07	-2	4.5 1.0	4.0 0.7	0.78
297-12	-5	2.0 1.1	2.9 0.9	0.50	350-09	1	3.8 1.5	3.4 1.0	0.69
297-32	1	2.1 1.1	2.4 0.9	0.91	350-19	3	4.1 1.4	3.6 1.0	0.13
297-34	-2	3.0 1.3	1.8 0.9	0.67	350-27	-2	3.2 1.5	4.6 1.1	0.64
298-16	3	4.0 1.0	3.8 0.7	0.24	350-28	-2	5.8 1.0	3.2 0.6	0.43
298-21	2	3.3 1.3	2.8 0.8	0.22	350-37	1	3.0 1.1	2.9 0.9	0.60
298-28	1	3.6 1.4	3.2 0.8	0.47	351-11	-2	4.8 1.5	3.4 0.9	0.33
299-20	1	2.9 1.2	4.4 0.8	0.45	351-16	11	3.6 1.2	9.9 1.0	0.55
301-12	1	4.6 1.4	3.1 1.1	0.82	351-20	0	4.0 1.5	4.8 1.0	0.54
302-18	1	1.6 1.3	3.3 0.8	0.31	351-23	1	3.8 1.0	3.2 1.0	0.70
303-05	9	5.9 1.7	4.2 1.4	1.00	351-25	3	2.3 1.2	4.0 1.0	0.58
303-10	-2	5.2 2.1	4.5 1.2	0.75	351-28	3	1.8 1.5	2.2 1.7	0.44
306-17	-2	5.7 1.3	5.9 1.0	0.63	352-02	3	3.1 0.5	2.3 0.4	0.45
324-16	-2	6.5 2.2	4.7 1.8	0.59	352-07	3	5.7 1.5	3.3 1.0	0.52
339-34	0	5.4 2.4	3.3 1.5	0.82	352-08	-2	1.8 1.3	1.9 1.1	0.59
340-03	-2	3.2 2.6	4.5 1.2	0.69	352-08	1	4.8 1.1	3.7 0.8	1.00
340-15	1	4.4 1.1	2.4 0.8	1.00	352-28	0	3.8 2.2	3.1 1.1	0.94
340-22	1	3.3 1.5	1.8 1.0	0.80	352-32	3	4.6 1.3	4.1 1.8	0.29
340-25	-2	4.3 0.7	6.0 1.2	0.85	352-38	-2	5.5 1.2	3.8 0.8	0.54
340-43	-2	2.9 1.2	4.5 0.8	0.92	352-41	1	3.9 0.8	4.7 0.6	0.56
341-04	9	2.8 0.5	7.7 0.4	0.60	352-44	-12	1.8 1.2	2.7 0.9	0.14
341-11	1	5.3 1.0	3.6 0.8	0.46	352-49	3	2.3 1.1	4.9 0.7	0.39
341-26	-2	4.1 1.0	1.7 0.8	0.55	352-51	-2	2.1 1.2	2.5 0.8	0.67
342-06	-2	4.9 1.4	3.9 1.1	1.00	352-54	4	7.0 1.9	4.1 1.3	0.13
342-08	-2	4.7 1.1	5.6 0.7	0.7	352-55	-2	3.8 0.9	3.9 0.6	0.75
342-19	-2	4.8 1.0	4.7 0.8	0.80	352-56	3	1.7 1.5	3.2 1.2	0.45
342-26	-2	5.7 0.5	4.4 0.8	0.50	352-62	3	2.0 1.7	2.7 0.9	0.11
342-27	-2	6.5 1.2	5.7 0.9	0.75	352-63	3	2.3 1.0	3.0 0.7	0.47
342-35	1	3.3 0.9	3.5 0.6	1.00	352-64	-2	1.9 1.0	3.0 0.7	0.21
342-38	-2	2.7 2.5	4.4 1.0	0.47	352-69	1	1.7 1.0	3.9 0.8	0.80
342-48	-2	1.3 1.1	2.2 0.8	0.46	352-71	3	4.5 1.2	3.2 0.9	0.50
343-11	-2	4.0 0.9	5.1 0.7	0.70	352-72	3	3.1 1.3	4.1 1.0	0.14
343-31	3	2.3 1.0	1.4 0.7	0.77	352-73	1	2.3 1.1	1.3 0.9	0.50
343-34	1	4.5 0.8	2.7 0.6	0.20	353-05	-2	4.0 0.9	3.0 0.7	0.60
344-16	3	2.3 0.6	1.0 0.6	1.00	353-07	2	2.1 0.3	1.7 0.3	0.83
345-10	-2	4.9 1.2	3.1 0.9	0.25	353-09	1	1.2 0.9	2.8 0.6	1.00
345-17	-2	3.4 1.6	3.8 1.0	0.38	353-16	3	3.2 1.9	5.4 1.6	0.70
345-24	-2	4.2 0.9	3.5 0.8	0.36	353-28	1	5.6 1.1	4.6 0.9	0.70
345-32	3	2.2 1.4	2.2 1.1	0.70	353-31	-2	5.6 0.9	3.4 0.8	0.18
346-03	-2	4.6 1.2	4.5 0.9	0.80	353-40	0	3.3 0.8	4.3 0.5	0.58
346-06	3	3.2 1.2	3.2 0.8	0.85	353-41	0	2.2 1.2	2.1 0.8	0.60
346-21	3	4.1 1.4	4.0 1.1	0.58	353-45	1	4.9 1.4	2.6 1.0	0.90

TABLE 3. (continued)

GALAXY ESO	TYPE	W(Mg I) $\pm \sigma$ (5175Å)	W(Na I) $\pm \sigma$ (5890Å)	b/a	GALAXY ESO	TYPE	W(Mg I) $\pm \sigma$ (5175Å)	W(Na I) $\pm \sigma$ (5890Å)	b/a
354-03	-2	2.5 1.2	3.3 0.7	0.80	401-27	1	2.7 2.1	2.8 1.1	0.36
354-05	3	1.4 1.4	3.0 1.0	0.13	401-23	3	5.5 1.4	4.8 1.1	0.80
354-09	3	2.3 1.4	4.5 1.0	0.42	401-24	1	3.5 1.1	3.1 0.9	0.82
354-12	-2	2.4 1.4	4.0 1.0	0.58	401-30	-2	4.6 1.3	4.4 1.1	0.90
354-19	3	4.2 1.2	2.9 1.0	0.58	402-02	-2	4.2 1.3	4.5 0.4	0.40
354-25	0	5.7 0.7	5.1 0.6	0.53	402-08	-2	2.9 1.0	3.8 0.8	0.60
354-26	-2	2.8 1.0	3.4 0.7	0.80	402-10	9	6.1 1.1	3.8 0.7	0.39
354-28	3	4.5 2.2	4.3 1.7	0.57	402-11	3	4.7 1.7	4.5 1.5	0.17
354-34	-2	4.1 0.9	3.1 0.7	1.00	402-14	-2	3.1 1.3	4.1 1.0	0.50
354-41	0	4.3 1.3	3.0 0.9	0.38	402-26	1	4.1 1.3	5.1 0.8	0.35
355-08	3	4.8 1.6	6.9 0.9	0.62	402-27	8	2.9 1.1	2.6 1.0	0.71
355-11	3	3.1 1.1	3.2 1.6	0.20	402-28	3	4.8 2.1	3.2 1.1	0.54
356-09	5	3.4 1.7	4.3 1.2	0.60	402-29	-2	2.7 1.4	3.9 1.0	0.20
356-11	9	3.4 1.3	4.0 1.2	0.29	403-03	1	4.8 2.1	2.6 1.3	0.07
356-14	9	4.8 1.0	4.8 0.6	0.16	403-06	3	2.7 1.2	2.3 1.0	0.40
357-09	-2	6.4 1.5	6.0 1.7	0.55	403-10	1	1.2 1.0	3.2 0.8	0.18
358-59	-5	2.5 0.9	1.7 0.7	0.67	403-12	1	5.3 1.0	3.5 0.7	0.94
360-09	1	4.9 1.1	3.9 0.9	0.70	403-22	-2	2.7 1.1	1.9 1.0	0.36
360-15	1	4.9 1.1	1.0 1.0	0.90	404-10	-2	3.3 1.2	4.7 0.9	0.25
361-06	1	4.1 1.3	2.1 1.2	0.91	404-15	1	1.2 1.2	2.2 0.8	0.27
361-16	1	3.4 1.0	3.9 0.8	0.93	404-39	-2	3.3 1.0	2.9 0.7	0.20
362-01	0	2.3 0.9	3.3 0.7	0.50	404-40	-2	3.4 1.3	5.0 0.8	0.43
362-08	0	2.1 0.7	3.7 0.5	0.46	404-45	5	4.8 1.6	3.9 0.9	0.09
362-22	3	3.3 2.0	2.5 1.8	0.58	405-09	1	3.2 1.5	4.4 0.2	0.50
363-02	3	3.6 1.6	5.0 1.4	0.36	405-11	1	2.0 1.2	4.7 0.8	0.43
382-03	3	3.9 1.5	3.3 1.1	0.75	405-15	8	2.6 0.8	1.6 0.7	0.89
382-16	-2	4.9 1.0	4.7 0.6	0.73	405-31	3	2.2 1.4	2.4 1.1	0.55
382-58	5	5.2 1.1	4.6 0.6	0.14	406-04	8	2.8 1.2	4.1 0.8	0.60
383-08	3	5.3 1.7	4.1 0.9	0.40	406-06	2	2.5 1.2	2.6 1.3	0.46
383-11	1	5.2 1.2	4.0 0.9	0.40	406-37	1	1.5 1.1	1.6 1.0	0.50
383-51	-12	2.7 1.8	4.7 0.9	0.20	407-03	1	5.6 2.5	4.5 2.7	0.70
383-76	-2	5.2 2.4	5.0 1.3	0.45	408-01	-2	4.8 1.0	2.7 0.9	0.22
384-07	-2	3.6 0.3	4.5 1.3	0.59	408-19	-2	3.2 1.1	2.8 1.1	0.64
384-09	5	2.7 1.8	3.9 1.2	0.71	408-20	1	7.1 1.7	5.1 1.1	0.64
384-14	-2	3.1 1.6	2.6 0.9	0.28	408-22	-2	4.7 1.2	4.4 0.9	0.67
384-19	-2	3.4 1.0	3.6 0.6	0.80	408-24	-3	4.8 1.1	5.4 0.7	0.60
384-21	-2	4.7 1.2	4.2 0.8	0.75	408-29	1	4.1 1.5	3.9 1.0	0.54
384-23	-2	3.2 1.0	3.5 0.8	0.42	408-31	1	4.9 2.3	4.7 1.1	0.39
384-26	-2	5.7 1.1	3.9 0.7	0.24	408-32	2	2.3 1.3	3.1 1.3	0.23
384-29	-2	3.5 1.1	2.5 0.6	0.87	408-34	-2	2.9 1.1	1.2 1.0	0.73
384-36	0	3.1 1.1	3.7 0.7	0.63	408-37	-3	4.6 1.0	3.7 0.7	0.93
384-49	-3	4.0 0.8	4.1 0.6	0.60	409-02	-2	4.2 1.2	3.5 0.8	1.00
384-51	-2	4.8 1.4	5.3 0.9	0.93	409-12	5	3.7 0.7	3.8 0.4	0.80
384-52	9	3.5 2.3	4.2 1.9	0.38	409-19	3	2.0 1.8	4.9 1.6	0.39
384-53	5	6.6 0.9	4.7 0.8	0.86	409-25	-5	1.8 2.7	7.1 2.3	0.53
384-59	1	4.5 2.1	4.6 1.3	0.43	411-28	-2	5.8 1.5	4.8 0.9	0.87
399-25	-2	4.6 1.1	3.1 0.7	0.46	411-33	1	2.9 1.5	2.9 0.9	0.36
400-04	1	2.7 1.5	3.4 1.0	0.67	412-16	7	3.2 1.8	2.7 1.0	0.45
400-06	1	3.4 0.9	2.1 0.7	0.80	412-17	1	5.7 1.6	2.2 0.9	1.00
400-13	-2	3.8 1.1	4.0 0.8	0.20	412-20	-2	3.6 0.9	4.8 0.8	0.55
400-17	5	3.5 2.5	3.3 1.2	0.35	412-27	3	5.9 1.8	5.7 1.0	0.10
400-33	3	2.8 1.3	3.5 1.1	0.30	413-05	-5	3.4 1.0	4.1 0.7	0.70
401-05	0	3.5 2.6	2.4 1.4	0.67	413-12	-2	4.3 1.5	2.4 1.0	0.64
401-06A	8	4.1 1.1	4.9 0.9	0.50	413-20	-2	2.9 0.7	3.0 0.6	0.21
401-06B	8	5.6 1.2	4.3 1.1	0.50	415-26	-2	1.8 1.1	4.7 0.7	0.41
401-08	-2	4.2 1.0	2.2 0.8	1.00	416-12	5	1.8 0.9	3.0 0.9	0.45
401-10	-2	3.6 1.1	3.1 0.8	0.50	416-18	-2	2.1 1.1	1.7 0.8	0.57
401-19	3	2.1 1.6	3.7 1.1	0.50	416-25	15	5.9 1.5	3.6 1.0	0.17

TABLE 3. (continued)

GALAXY ESO	TYPE	W(Mg I) $\pm \sigma$ (5175Å)	W(Na I) $\pm \sigma$ (5890Å)	b/a	GALAXY ESO	TYPE	W(Mg I) $\pm \sigma$ (5175Å)	W(Na I) $\pm \sigma$ (5890Å)	b/a
416-35	1	2.7 1.6	3.6 0.8	0.86	462-09	1	1.4 1.2	2.0 0.9	0.77
416-39	-2	3.7 1.1	4.7 0.8	0.80	462-11	1	4.3 1.8	2.2 1.3	0.46
416-40	3	1.4 1.2	1.6 0.9	0.67	462-15	-5	5.0 1.0	4.6 0.8	0.77
416-41	3	2.9 1.3	2.4 0.9	0.36	462-21	-2	5.0 1.0	4.9 0.9	0.31
417-01	1	4.2 1.1	4.4 0.8	0.46	462-26	-2	1.2 1.3	3.5 0.9	0.50
417-02	-2	5.6 1.1	4.2 0.8	0.36	463-01	-2	3.8 1.5	4.3 1.1	0.73
417-06	-2	4.1 1.0	3.2 0.7	0.83	463-11	-2	3.9 1.3	3.0 1.1	0.33
417-21	-3	2.3 1.1	5.3 0.7	0.54	463-25	3	3.6 1.3	2.5 0.9	0.11
418-11	1	3.7 1.3	3.7 0.8	0.70	464-05	1	3.9 1.3	3.3 0.8	0.76
419-06	3	3.0 1.3	3.5 1.3	0.91	464-17	-3	3.5 2.2	4.1 1.0	0.54
420-17	-2	1.5 1.0	2.9 0.7	0.28	465-04	-2	2.8 1.5	2.5 1.0	0.86
422-23	3	4.0 1.1	3.9 0.9	0.52	466-03	1	2.8 1.4	4.6 0.8	0.40
422-24	3	4.7 1.4	6.3 1.4	0.42	466-26	-5	3.7 0.9	3.4 0.7	0.73
423-13	3	5.1 1.4	3.7 1.0	0.24	467-37	-3	2.9 0.7	5.3 0.6	0.53
438-20	3	1.3 1.3	5.4 0.8	0.60	467-46	-2	3.4 0.9	4.2 0.7	0.90
438-23	-12	4.2 1.2	4.9 0.8	0.60	467-54	-2	3.4 1.4	5.2 0.8	0.44
439-18	3	3.0 1.2	4.0 0.8	0.76	467-58	11	2.1 1.8	5.0 1.0	0.40
439-20	3	2.2 1.5	3.6 1.0	0.41	468-01	-2	5.1 0.8	3.2 0.6	0.33
440-25	-2	4.9 1.0	4.8 0.8	0.73	468-16	-2	3.1 0.9	4.3 0.8	0.55
440-32	-2	3.6 1.3	2.9 0.8	0.43	468-17	1	3.9 1.2	2.3 1.0	0.31
440-38	1	2.4 1.2	2.0 0.8	0.59	469-07	3	3.9 1.6	2.7 1.3	0.58
442-03	-3	4.2 1.2	4.3 0.8	0.67	470-14	1	4.6 1.4	3.5 1.0	0.72
442-06	-2	4.8 1.1	4.1 0.8	1.00	471-07	0	5.7 1.3	3.4 1.1	0.58
443-24	-5	3.5 0.9	3.9 0.6	0.88	471-32	-2	4.2 1.0	2.2 0.7	0.68
443-31	0	4.3 1.3	5.3 0.7	1.00	471-34	1	4.2 1.4	2.7 0.8	0.77
443-32	-5	3.5 1.0	3.9 0.6	0.78	471-45	-5	3.3 1.4	3.8 0.8	0.77
443-39	-2	2.5 1.0	3.8 0.6	0.56	473-16	1	4.3 1.4	3.5 0.8	0.50
443-43	-2	3.0 1.0	2.5 0.6	0.93	474-36	-2	2.2 2.9	2.8 0.9	0.69
443-52	0	3.2 1.2	3.7 0.7	0.36	481-17	1	3.0 1.4	2.5 0.8	1.00
443-53	-5	2.5 1.5	3.1 0.8	0.80	481-22	1	3.1 1.8	2.7 0.7	0.80
443-55	-2	3.5 2.1	2.7 1.0	0.93	482-18	-2	4.0 1.4	2.1 0.9	1.00
443-56	1	3.5 1.5	2.1 1.2	0.58	483-13	1	2.4 1.4	1.1 1.0	0.50
443-66	0	1.5 1.4	4.4 1.2	0.80	485-16	1	2.7 2.0	4.2 0.8	0.32
443-77	-2	3.4 1.2	2.4 0.7	0.20	486-04	1	3.7 1.6	1.8 0.9	0.50
444-12	3	3.5 1.2	2.3 0.9	0.94	486-23	-2	4.5 1.8	5.4 0.9	1.00
444-18	-2	2.9 1.4	6.9 0.8	0.71	503-05	3	4.0 1.3	3.4 0.8	0.87
444-25	-2	6.5 1.1	4.2 0.8	0.58	507-14	0	2.9 0.9	4.6 0.6	0.53
444-46	-2	6.3 1.6	5.8 1.1	0.57	507-21	-2	5.1 0.7	4.7 0.6	0.35
444-71	0	5.2 2.0	3.6 1.2	0.35	508-08	-2	7.2 1.1	5.0 0.7	0.87
444-87	1	5.7 1.2	2.1 0.8	0.75	508-72	1	5.8 1.0	3.4 0.7	0.38
445-01	-2	5.5 1.1	4.6 0.7	0.58	509-03	-2	4.4 1.4	4.1 0.9	0.44
445-05	2	2.9 2.8	3.0 1.3	0.62	509-08	-2	2.8 1.1	5.0 0.7	0.53
445-14	1	5.3 1.9	4.4 1.1	0.50	509-12	-2	5.3 1.3	4.6 1.1	0.91
445-15	3	6.2 1.0	3.0 0.8	0.37	509-19	5	4.6 1.6	6.4 1.0	0.09
445-27	5	4.5 1.9	3.2 1.3	0.56	509-98	0	5.8 1.4	5.4 1.1	0.77
445-28	-2	3.0 0.8	5.5 0.5	0.80	509-108	-2	4.3 1.4	3.9 0.9	0.35
445-42	0	2.6 1.0	3.4 0.7	0.15	510-10	1	3.8 1.1	4.3 0.6	0.73
445-49	-12	4.2 1.3	3.8 0.7	0.42	510-11	1	4.2 1.3	3.0 0.8	0.47
445-51	1	4.5 1.3	4.4 0.9	0.53	510-46	1	3.5 1.2	3.2 0.8	0.88
445-52	-2	4.9 1.0	2.4 0.6	0.73	510-54	-3	3.9 0.8	5.0 1.1	0.69
445-59	-5	3.6 0.9	4.0 0.6	0.50	510-56	1	4.7 2.1	4.4 1.1	0.80
445-64	-2	3.0 1.3	5.5 0.7	0.92	511-21	-5	5.6 0.2	5.6 0.8	0.58
445-65	-2	2.1 1.0	3.9 0.7	0.11	511-23	-2	5.4 1.3	4.4 0.8	0.69
445-69	1	3.4 1.1	3.4 0.7	0.50	511-31	2	2.7 1.4	3.1 0.9	0.61
445-73	1	1.9 1.1	5.1 0.7	0.57	511-32	0	1.4 1.2	3.5 0.8	0.78
445-75	-2	4.9 1.5	2.8 0.8	0.60	528-08	-2	4.2 1.4	5.4 0.7	1.00
446-01	3	5.0 1.1	2.4 0.9	0.63	528-23	1	1.7 1.2	2.4 0.7	0.42
446-03	-2	4.8 1.0	4.9 0.7	0.67	530-18N	1	3.4 2.6	3.4 1.3	0.27
446-17	3	3.9 0.9	2.4 0.7	0.69	530-18S	1	6.2 2.1	3.7 1.2	0.27

TABLE 3. (continued)

GALAXY ESO	TYPE	W(Mg I) ± σ (5175Å)	W(Na I) ± σ (5890Å)	b/a	GALAXY ESO	TYPE	W(Mg I) ± σ (5175Å)	W(Na I) ± σ (5890Å)	b/a
530-24	-2	4.8 1.4	3.0 0.9	0.20	548-44	1	2.5 1.1	1.3 0.7	0.47
530-30	1	5.3 1.5	4.5 0.8	0.93	548-47	1	4.7 1.0	3.4 0.6	0.22
530-33	-2	4.2 1.3	2.2 0.8	1.00	548-68	-2	4.5 1.3	2.2 0.7	0.44
531-02	1	5.4 1.7	5.4 1.0	0.89	548-75	4	5.4 2.7	2.6 1.3	0.73
531-18	-3	6.7 1.1	4.5 0.7	0.90	548-79	1	3.7 1.3	2.4 0.8	0.89
533-04	5	3.7 1.4	2.9 1.1	0.18	548-81	0	4.5 1.3	4.7 0.7	0.87
533-09	-2	4.8 1.3	3.1 0.8	0.83	549-40	4	3.3 1.2	3.8 0.7	0.37
533-20	-3	4.0 1.6	6.2 1.0	0.57	550-02	3	4.7 1.7	2.9 0.9	0.20
533-21	-3	3.0 0.7	3.8 0.5	0.57	552-04	0	4.3 1.2	3.0 0.6	0.86
533-26	3	4.1 0.3	2.7 1.3	0.33	552-09	4	2.7 1.6	1.5 1.3	0.80
534-02	-5	4.2 1.3	4.8 0.7	0.58	552-11	-2	1.8 1.8	5.7 1.0	0.22
534-06	-2	4.7 1.3	3.1 0.8	0.67	552-20	-3	4.7 1.9	4.7 1.0	0.59
536-02	0	4.8 1.1	3.8 0.7	0.67	552-27	-2	5.1 1.2	4.5 0.7	1.00
538-10	-2	4.2 1.0	3.7 0.7	0.92	552-40	1	5.7 1.1	2.7 0.7	0.63
538-11	3	2.2 2.5	2.2 1.6	0.69	552-45	1	6.7 1.7	4.6 0.8	0.53
538-13	1	3.8 1.5	5.1 0.8	0.50	552-52	-3	3.6 1.1	2.2 0.5	0.75
538-14	1	2.1 1.5	1.9 1.0	0.57	553-18	1	4.2 1.6	3.8 0.8	0.79
538-23	1	3.7 1.4	4.2 0.9	0.77	596-46	-2	4.7 1.7	3.5 1.0	0.69
538-25	-2	3.5 1.8	2.7 1.2	0.22	596-48	-5	5.2 1.0	3.2 0.7	0.60
540-03	1	2.4 0.9	2.0 0.5	0.43	597-01	-2	5.6 1.2	4.4 0.8	0.67
540-09	3	4.2 1.4	1.8 1.4	0.60	597-04	-2	1.3 1.4	4.4 0.9	0.47
540-17	1	5.1 1.8	4.8 1.1	0.29	597-06	-2	3.2 1.4	5.7 0.9	0.86
541-07	-3	5.2 2.8	5.8 0.1	0.86	597-23	-2	3.4 1.0	6.3 0.6	0.83
541-13	-3	5.8 2.0	4.6 0.8	0.65	597-26	-2	4.0 1.2	4.5 0.8	1.00
541-25	4	2.1 1.7	2.4 1.0	0.60	597-27	1	3.9 1.7	2.2 1.1	0.62
542-06	-2	3.7 1.0	4.1 0.6	0.56	597-35	3	6.8 2.0	4.3 0.9	0.30
542-13	-3	3.2 0.9	3.9 0.6	0.83	597-36	13	5.8 2.5	5.1 1.0	0.17
542-15	-2	3.1 1.0	3.2 0.6	1.00	597-41	1	4.0 2.1	3.2 1.1	0.59
543-12	3	3.2 1.6	3.3 0.9	0.47	598-03	-2	4.7 1.5	3.2 0.9	0.69
543-20	1	5.7 1.4	3.8 0.8	0.52	598-14	-2	6.1 2.1	3.2 1.2	0.50
543-26	3	6.4 1.1	4.0 1.9	0.53	598-31	-2	4.8 1.1	4.8 0.7	0.75
545-05	9	2.0 1.1	2.6 1.0	0.35	599-04	0	5.2 1.7	3.7 1.0	0.53
545-26	3	4.3 1.1	3.0 0.9	0.88	599-15	4	3.6 1.6	4.2 1.0	0.50
545-40	-2	5.1 1.0	2.0 0.5	0.61	600-01	1	3.3 0.6	3.3 0.1	0.38
545-42	-2	2.3 1.3	0.7 0.8	0.44	600-04	-2	4.8 1.2	3.1 0.7	0.88
546-08	1	3.2 0.9	1.6 0.5	0.86	603-29	-2	4.6 1.3	3.3 0.9	0.50
546-28	3	2.9 1.1	2.5 0.7	0.92	605-03	1	2.4 1.0	3.7 0.6	0.18
548-33	0	3.0 1.5	2.8 0.8	0.50					

south to $\delta = -17.5^\circ$ have been taken from *The ESO/Uppsala Survey of the ESO (B) Atlas* (Lauberts 1982).

The morphological types are coded as follows: $-5 = E$; $-3 = E/SO$, $-2 = SO$; $0 = SOa$; $1 = Sa$; $2 = Sab$; $3 = Sb$; $4 = Sbc$; $5 = Sc$; $6 = Sd$; and $9 =$ interacting systems.

Special attention was given to galaxies with dust lanes. In the previous tables they appear with an extra "1" preceding the code for its morphological type.

For galaxies north to $\delta = -17.5^\circ$, we have used the data given by the *Uppsala General Catalogue of Galaxies* (Nilson 1973), or the *Second Reference Catalogue of Bright Galaxies* (de Vaucouleurs et al. 1976).

3. DISCUSSION

In this section we analyze the behavior of the $W(\text{Na I})$ × $W(\text{Mg I})$ plane for separated classes of morphological

types of galaxies and the effects caused by different galaxy inclinations in a given class.

The elliptical galaxies of the sample are plotted in Fig. 2. There is a correlation between $W(\text{Mg I})$ and $W(\text{Na I})$. The linear regression excluding the two deviating points (discussed below) is $W(\text{Na I}) = 0.48 (\pm 0.022) W(\text{Mg I}) + 2.30$ and has $r = 0.51$. We interpret this relation as the effect of metallicity for galaxy nuclei dominated by old stellar populations, which in turn is a function of luminosity (Faber 1973; Bica & Alloin 1987). The error ϵ for the declivity parameter in the latter regression, as well as for the subsequent ones, were calculated using the following relation (see Press et al. 1989):

$$\epsilon^2 = \frac{\sum_{i=1}^N 1/\sigma_{y_i}^2}{\sum_{i=1}^N 1/\sigma_{y_i}^2 \sum_{i=1}^N x_i^2/\sigma_{x_i}^2 - (\sum_{i=1}^N x_i/\sigma_{x_i}^2)^2},$$

where σ_{y_i} and σ_{x_i} are standard deviations of the $W(\text{Na I})$

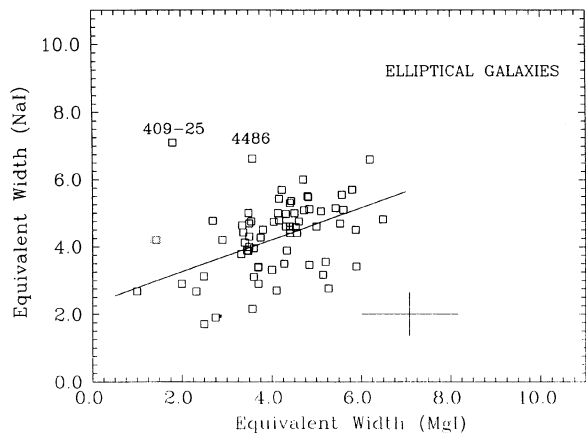


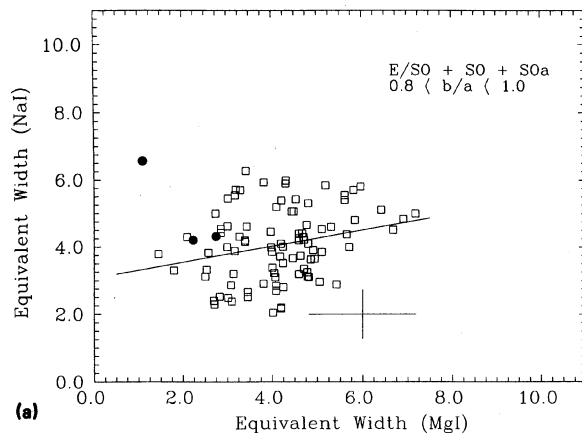
FIG. 2. Plane $W(\text{Na I}) \times W(\text{Mg I})$ for a sample of southern elliptical galaxies. In the horizontal axis is plotted the equivalent width for the Mg I ($\lambda 5175 \text{ \AA}$) absorption line. The vertical axis is the equivalent width for Na I ($\lambda 5893 \text{ \AA}$). The straight line shows the linear regression calculated excluding the two deviating points at the upper left, which correspond to ESO 409 G25 (at left) and NGC 4486 (M87, at right). The error bars represent the mean errors in the determination of equivalent widths.

and $W(\text{Mg I})$, respectively (Tables 1–3).

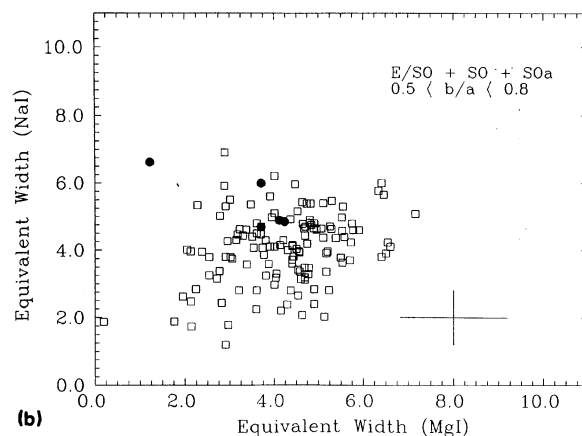
The two deviating points correspond to NGC 4486 (M87), which is a dominant elliptical galaxy in the Virgo cluster, and to ESO 409 G25 which, according to the *ESO/Uppsala Catalogue* (Lauberts 1982) is also a dominant galaxy in a cluster. Considering that M87 (also known as the radiosource Virgo A) has ionized gas in the nuclear region (see, e.g., Walker & Hayes 1967), the Na I excess with respect to the regression could be associated to the presence of interstellar gas in the nuclear region of both galaxies.

The sample of lenticular galaxies plus intermediate groups E/SO and SO/Sa has been divided into three axial ratio intervals as shown in Figs. 3(a)–3(c). The axial ratio is basically an indicator of galaxy inclination. The face-on lenticulars [Fig. 3(a)] have a distribution similar to that of the elliptical galaxies. For moderately inclined lenticulars [Fig. 3(b)] deviating points with Na I excess are more frequent than in Fig. 3(a). In addition, the largest deviations are exactly dust lane galaxies. Finally, for the most inclined lenticulars [Fig. 3(c)] the largest $W(\text{Na I})$ values are associated to galaxies with dust lanes originating from the nearly edge-on disks. This indicates that interstellar gas from the disks would be responsible for the large Na I excess. The linear regressions for Figs. 3(a) and 3(c) are, respectively $W(\text{Na I}) = 0.24 (\pm 0.028) W(\text{Mg I}) + 3.07$ with $r = 0.49$, $W(\text{Na I}) = 0.18 (\pm 0.033) W(\text{Mg I}) + 3.10$ with $r = 0.45$. Consequently the correlation for the ellipticals (see Fig. 2) or to face-on lenticulars [Fig. 3(a)] deteriorates for the inclined lenticulars [Fig. 3(c)]. A possible explanation would be the contamination of the nuclear light by the line-of-sight contribution from younger population of the disks, in addition to the Na I excess due to the gas.

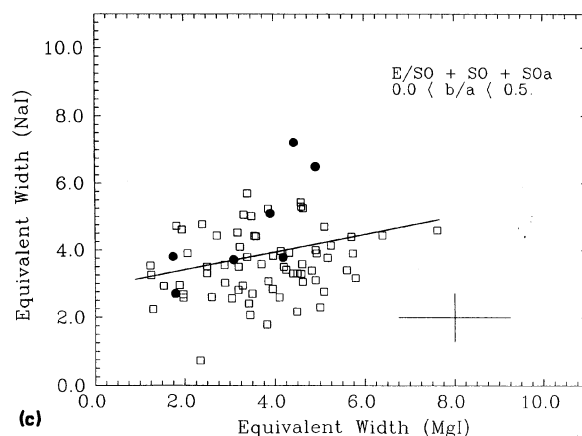
In Fig. 4 we illustrate all early type spirals (Sa and Sab) available in the sample. Note that there is a similar distribution to that of elliptical galaxies. In fact the stellar populations in bulges of early type spirals are in most cases similar to those of ellipticals (Bica 1988). The deviating points are



(a)



(b)



(c)

FIG. 3. (a) Same as Fig. 2, but for a sample of lenticular galaxies with inclinations in the range $0.8 < b/a < 1.0$. Black circles represent systems with dust absorption lanes. (b) Same as Fig. 2, but for a sample of lenticular galaxies with inclinations in the range $0.5 < b/a < 0.8$. Black circles as in (a). (c) Same as Fig. 2, but for a sample of lenticular galaxies with inclinations in the range $0 < b/a < 0.5$. Black circles as in (a).

again associated to very inclined systems, as in the case of the lenticular galaxies.

The late type spirals have been divided into three axial ratio intervals, as shown in Figs. 5(a)–5(c). The lower envelope of the distributions increases from $W(\text{Na I})$ about 1.0 \AA

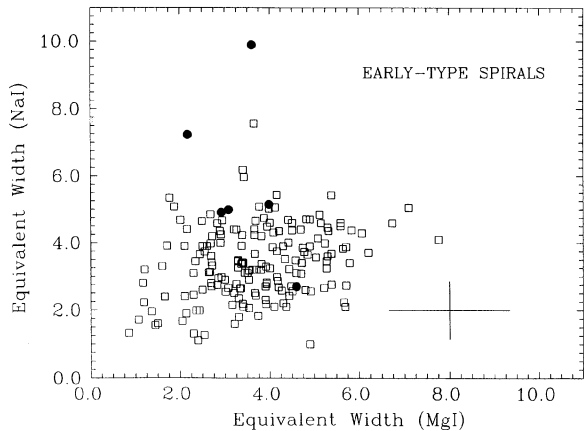
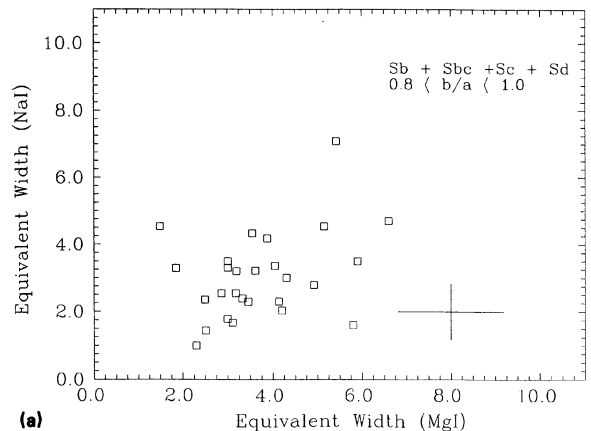


FIG. 4. Same as Fig. 2, but for a sample of early type spiral galaxies (Sa and Sab). Black circles as in Fig. 3(a).

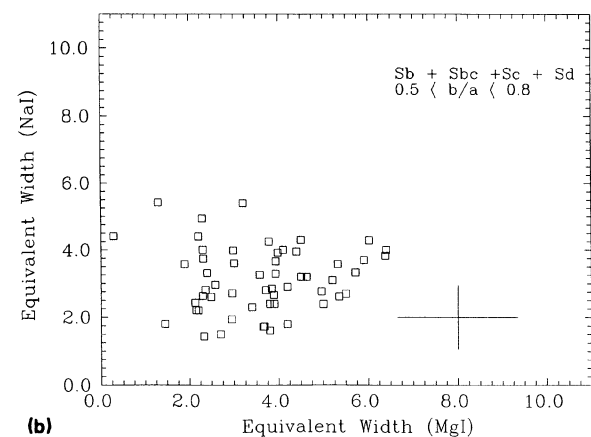
for face-on galaxies up to 2.0 \AA for the nearly edge-on objects. In addition, the number of points above $W(\text{Na I})$ about 4 \AA increases significantly for the more inclined galaxies ($0 < b/a < 0.5$). A natural explanation is that in late spirals the disk thickness is similar to the bulge diameter and, consequently, the interstellar Na I absorption is pronounced. As the bulges are small in late type spirals, they do not present the line strength correlation Na I vs Mg I not even for the face-on sample [Fig. 5(a)]. This correlation is clear for the bulge dominated galaxies (Fig. 4). The absence of correlation for late type spirals is certainly due to the relatively large contribution by the blue disk population and also because quite often this type of galaxy presents nuclear blue population (Bica 1988). Indeed the continuum of the blue population dilutes more the Mg I at 5175 \AA than Na I at 5890 \AA , populating the region $3 \text{ \AA} < W(\text{Na I}) < 5 \text{ \AA}$ and $1 \text{ \AA} < W(\text{Mg I}) < 4 \text{ \AA}$ as shown in Fig. 5(a).

The sodium excesses in the late type spirals are in many cases as large as $\Delta W(\text{Na I}) \approx 3 \text{ \AA}$ with respect to the mean value in their face-on counterparts. Comparable excesses are observed for early type galaxies with dust lanes with respect to their normal counterparts. This coincidence not necessarily implies similar gas amounts. In the inclined spirals we observe an equivalent width excess arising from the gas clouds of the disk, affected by its kinematics and eventual saturation effects in individual clouds, which might give an indication of column densities. In turn in the dust lane E and SO's the gas column densities are certainly smaller, but the metal abundance in the central region of giant E and SO galaxies is higher than in spiral disks, which might produce similar $W(\text{Na I})$ excesses.

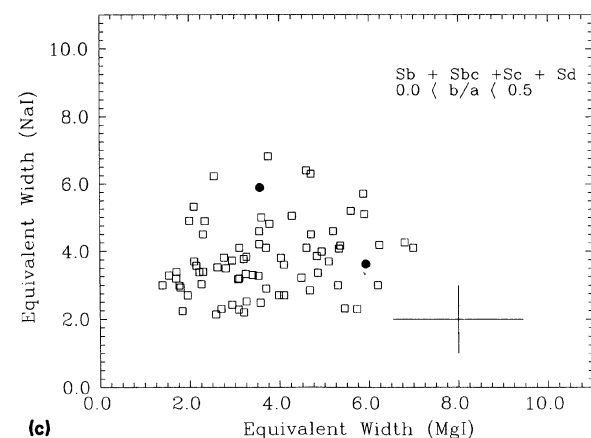
The effects discussed in this section can be visualized in Fig. 1 by comparing the Na I strength to that of Mg I. The galaxy ESO 541 G13 represents a typical stellar population of an E-SO galaxy nucleus without detectable interstellar Na I. NGC 5078 is an SO galaxy with dust lanes. Notice the Na I excess relative to Mg I. NGC 3717 is a very inclined ($b/a = 0.26$) spiral galaxy with red stellar population. In this system, the interstellar Na I contribution is important. Finally, NGC 1808 is an inclined ($b/a = 0.5$) spiral with strong interstellar Na I. In addition the nucleus has young stellar components which dilute the Mg I lines, exacerbating the difference between Na I and Mg I.



(a)



(b)



(c)

FIG. 5. Same as Fig. 2, but for a sample of late type spiral galaxies (Sb to Sd) with inclinations in the range $0.8 < b/a < 1.0$. (b) Same as Fig. 2, but for a sample of late type spiral galaxies (Sb to Sd) with inclinations in the range $0.5 < b/a < 0.8$. (c) Same as Fig. 2, but for a sample of late type spiral galaxies (Sb to Sd) with inclinations in the range $0 < b/a < 0.5$.

4. CONCLUSIONS

Our main results may be summarized as follows:

- (1) Most of early type galaxies with dust lanes present an enhancement of the Na I absorption line ($\lambda 5893 \text{ \AA}$).
- (2) Spiral galaxies tend to show a displacement toward

higher values of the equivalent width of the Na I line as a function of inclination (b/a). This result, previously obtained for a sample with $V \leq 6000 \text{ km s}^{-1}$, is now found to be also present for a larger sample reaching larger distances (up to $V \leq 25\,000 \text{ km s}^{-1}$).

(3) As, on average, we are observing more distant systems, the slit covers a large bulge fraction rather than the very nucleus. The persistence of the effect mentioned in (2)

suggests that the scale height of the gas layer in the central disk can reach a considerable fraction of the bulge radius.

We would like to thank Dr. L. N. da Costa for allowing us to use the information of the SSRS data bank in this article, and also to the Brazilian institution CNPq for grants that partially have supported this work.

REFERENCES

- Bica, E. L. D., and Alloin, D. 1986, *A&A*, 166, 83
 Bica, E. L. D., and Alloin, D. 1987, *A&A*, 181, 270
 Bica, E. L. D. 1988, *A&A*, 195, 76
 Cohen, J. 1973, *ApJ*, 186, 149
 da Costa, L. N., Pellegrini, P. S., Nunes, M. A., Willmer, C., and Latham, D. W. 1984, *AJ*, 89, 1310
 da Costa, L. N., Pellegrini, P. S., Willmer, C., de Carvalho, R., Maia, M., Latham, D. W., and Geary, J. C. 1989, *AJ*, 97, 315
 de Vaucouleurs, G., de Vaucouleurs, A., and Corwin, Jr., H. G. 1976, *Second Reference Catalogue of Bright Galaxies* (University of Texas Press, Austin)
 Faber, S. 1973, *ApJ*, 179, 731
 Hobbs, L. 1974, *ApJ*, 191, 381
 Lauberts, A. 1982, *The ESO/Uppsala Survey of the ESO (B) Atlas* (European Southern Observatory, Garching)
 Press, W. H., Flannery, B. P., Teukolsky, S. A., and Vetterling, W. T. 1989, *Numerical Recipes, The Art of Scientific Computing* (Cambridge University Press, Cambridge), p. 504
 Nilson, P. 1973, *Uppsala General Catalogue of Galaxies* (Royal Society of Sciences, Uppsala)
 Spitzer, L. 1948, *ApJ*, 108, 276
 Walker, M., and Hayes, S. 1967, *ApJ*, 149, 481